Novel schemes to generate multi-level modulation formats for ultra-capacity coherent detection transmission systems

(Invited Paper)

Jianjun Yu[1]* and Xiang Zhou[2]**

[1] *ZTE USA Inc., Iselin, NJ 08830, USA, and also with ZTE Inc., Beijing 100876, China*

[2] *AT&T Labs–Research, Middletown, NJ 07748, USA*

* *E-mail: yu.jianjun@zte.com.cn;* ** *e-mail: zhoux@research.att.com*

Received June 2, 2010

We summarize several novel schemes to generate multi-level modulation formats for high capacity transmission system with high spectral efficiency. We show that multi-level 8QAM, 16QAM, 32QAM, and 64QAM (QAM: quatlrature amplitude modulation) optical signals can be generated by commercial optical and electrical devices. Employing these multilevel modulation formats, we have realized PDM-8QAM (PDM: polarization division multiplexing) 32 Tb/s and PDM-36QAM 64-Tb/s signals transmission over 580- and 320-km fibers, respectively.

OCIS codes: 250.0040, 250.4110, 250.4480, 250.5530, 190.4370.

doi: 10.3788/COL20100809.0823.

1. Introduction

To increase the fiber capacity, spectrally-efficient modulation formats and coherent detection technologies have been extensively explored in the research community. By employing multi-level modulation formats, new record of spectral efficiency for 100-Gb/s optical signal has been built. In 2008, we set up the spectral efficiency record of 4 (bit/s)/Hz with PDM-8PSK (PDM: polarization division multiplexing, PSK: phase shift keying)[1,2], and in 2010 we built another record of spectral efficiency of 8 (bit/s)/Hz by using PDM-36QAM modulation format for 100-Gb/s signal[3]. By using these novel modulation formats, the record of the transmission capacity is built. Up to now, the highest capacity record is 69.1 Tb/s by using 16QAM with spectral efficiency of 6.4 (bit/s)/Hz[4]. Table 1 summarizes the transmission capacity.

The rest of this paper is organized as follows. In Section 2, we describe the proposed high-speed multi-level modulation schemes, including 8QAM, 16QAM, 36QAM, and 64QAM. Section 3 is devoted to the ultra-high capacity and single-channel high bit rate transmission systems. Finally we present the conclusions in Section 4.

2. Novel schemes to generate multi-level modulation formats

The demonstrated highest spectral efficiency of quadrature phase shift keying (QPSK) modulation is limited to be 4 (bit/Hz)/s[5]. In order to further improve the spectral efficiency, multi-level modulation formats such as 8PSK, 8QAM, 16QAM, 32QAM, and 64QAM can be employed. Relative to 8QAM, 8PSK is worse at receiver sensitivity, so we do not discuss how to generate 8PSK in this paper. In the following sections, we will demonstrate how to generate these multi-level modulation format signals by using commercial products.

2.1 8QAM format

In theory, PDM-8QAM can tolerate 1.6 dB more noise than PDM-8PSK[5−10] because it encodes the signal in all four dimensions of an optical carrier, and is probably the optimal 64-ary modulation format. Although 8QAM signal can be easily generated by an electrical arbitrary waveform generator (AWG), it is quite difficult in generating in pure optical scheme. Generation of an 8QAM optical signal is not as straightforward as 8PSK because both the phase and the amplitude have to be modulated in a coordinated way.

In Ref. [6], we experimentally generated 114-Gb/s PDM-8QAM optical signal using a commercial dual-parallel Mach-Zehnder modulator (MZM) followed by a common phase modulator (PM) with binary electrical driving signal through a novel synthesis technique. The operational principle of the proposed 8QAM modulator is shown in Fig. 1(a). The 8QAM modulator consists of a parallel in-phase/quadrature (I/Q) modulator plus a $(0, \pi/2)$ PM. For the parallel I/Q modulator, the phase

Table 1. Some Current High Capacity Transmission Beyond 1 Tb/s

Ref.	Bit Rate/ Channel (Gb/s)	Spectral Efficiency ((bit/Hz)/s)	Capacity (Tb/s)	Modulation Format
[4]	171	6.2	69.1	PDM-16QAM
[3]	107	8	64	PDM-32QAM
[6]	114	4	32	PDM-8QAM
[7]	160	3.2	25.6	PDM-RZ-DQPSK
[1]	114	4	17	PDM-RZ-8PSK
[8]	112	2	16.4	PDM-QPSK
[9]	114	4	16.0	PDM-8QAM

RZ: return-to-zero.

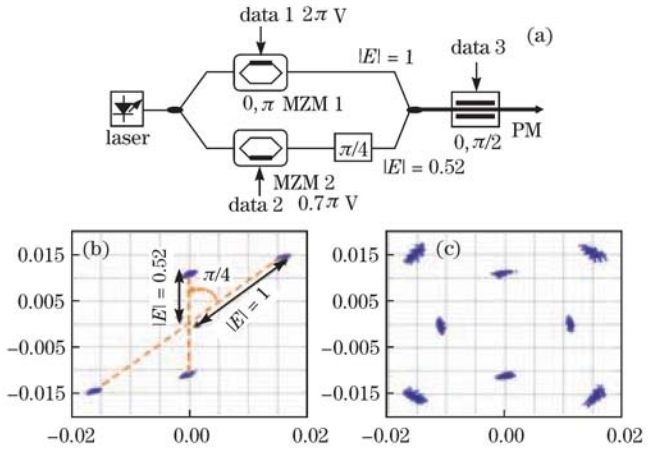

Fig. 1. (a) Proposed 8QAM transmitter; simulated constellation diagrams (b) after the parallel I/Q modulator and (c) after the (0, $\pi/2$) phase modulator. $|E|$ denotes the relative amplitude of the optical field.

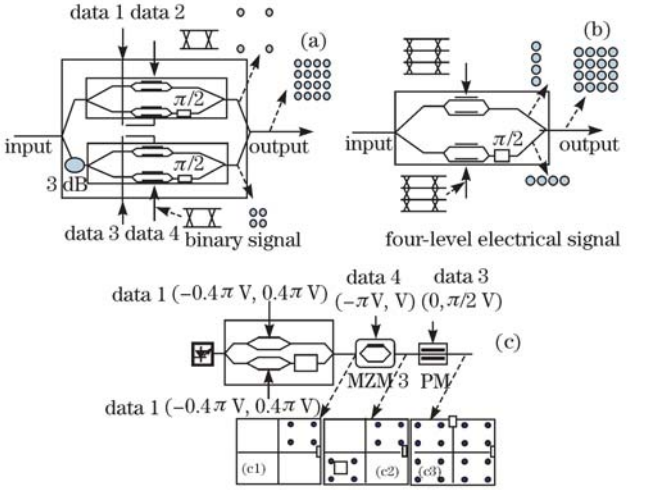

Fig. 2. Illustration of the proposed 16QAM modulator. (a) Quad-parallel MZM with binary drive signals, (b) I/Q modulator driven by four-level electrical, and (c) commercial modulators with binary driving signals through a novel synthesizing method.

difference between the upper and the lower branch is set to be $\pi/4$. This is different from the conventional operation where the phase difference is ideally $\pi/2$. The two parallel MZMs (MZM1 and MZM2) are both biased at the null point but with different drive voltages: MZM1 is driven with a full 2π-V peak-to-peak signal while MZM2 is only driven with a 0.7π-V swing. As a result, the parallel I/Q modulator introduces both amplitude and phase modulation (with amounts we required) to the original continuous-wave (CW) signal as shown in Fig. 1(b), where we give the simulated constellation diagram at the output of the parallel I/Q modulator. After introducing (0, $\pi/2$) phase modulation, an optimal circular 8QAM signal is generated, as shown in Fig. 1(c).

2.2 16QAM format

16QAM has been proposed and generated in different methods[11−13] such as 16QAM generation based on AWG and parallel I/Q modulators. 50-Gb/s 16QAM was generated using a special quad-parallel MZM with binary drive signals[4,12], as shown in Fig. 2(a), and 112-Gb/s PDM-16QAM has been generated using four-level electrical driving signals and parallel I/Q modulators[11], as shown in Fig. 2(b). In Ref. [13], we demonstrated that rectangular 16QAM can also be generated using commercial modulators with binary driving signals through a novel synthesizing method. The operational principle of the proposed high-speed rectangular 16QAM modulator is shown in Fig. 2(c)[13]. It consists of a pair of $\pi/2$-biased dual-parallel MZMs (i.e., MZM1 and MZM2), a common (0, π) MZM (i.e., MZM3), and a (0, $\pi/2$) PM. For the $\pi/2$-biased dual-parallel MZM, both MZM1 and MZM2 are biased at 0.6π V with a peak-to-peak drive swing of 0.8π V. Such a driving condition will result in an offset rectangular 4QAM constellation as shown in Fig. 2(c1). We then pass this offset rectangular 4QAM signal through a (0, π) MZM (biased at the null point with a peak-to-peak driving swing of 2π V) to generate a special 8QAM constellation, as shown in Fig. 2(c2). Finally we pass this special 8QAM signal through a (0, $\pi/2$) PM, and then we can obtain a standard rectangular 16QAM signal as shown in Fig. 2(c3). Note that the results shown in Fig. 2(c) are all based on numerical simulation by assuming that all the MZMs and the PM (including the electrical driving circuitry) have a first-order Gaussian filter response function with a 3-dB bandwidth equal to 70% of the symbol rate. Because we only use binary electrical driving signals, the proposed method has the potential to generate very high speed rectangular 16QAM signals for 100 Gb/s and above optical transmission applications by using commercially available modulators.

2.3 36QAM format

Behind 16QAM, the modulation format should be 32QAM. If a CW lightwave is modulated by a parallel modulator (I/Q modulator) driven by six-level (bit) electrical signals which are generated from a commercial AWG, 36QAM optical signal is generated. In order to generate 32QAM optical signal, some special operation will be required. It means that the highest level electrical I and Q signals cannot be used to drive the parallel modulator simultaneously. For simplification, we only discuss how to generate 36QAM optical signal with high performance. In our experiment, the 36-QAM optical signal is generated by driving an I/Q modulator with a 10.7 Gbaud. 36QAM baseband signal obtained from a commercial AWG running at 21.4 GSa/s[3]. The current bandwidth of commercial AWG is only 7.5 GHz. We operate the AWG in the interleaving mode to achieve such a high sampling rate: the analog output (six-level signals with pseudo-random pattern length = 2^{15}) and its delayed inverse copy are used as the I and Q components, respectively. We compare the constellation with post-equalization and with pre-equalization of deterministic transmitter filtering effects due to the limited bandwidth of AWG as shown in Figs. 3(b) and (d), respectively. We can see that using both pre-equalization and post equalization is better than purely post-equalization because post-equalization will enhance noise components

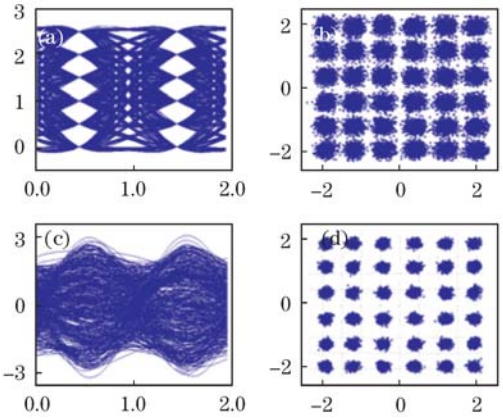

Fig. 3. (a) Electrical waveform from one port of AWG without pre-equalization; (b) optical constellation with post-equalization; (c) electrical waveform from one port of AWG with pre-equalization; (d) optical constellation with both pre-equalization and post-equaliztion.

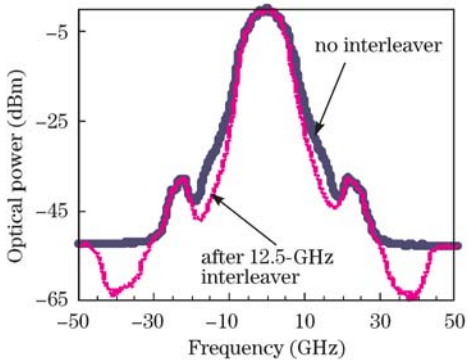

Fig. 4. Optical spectra before and after 12.5-GHz interleaver.

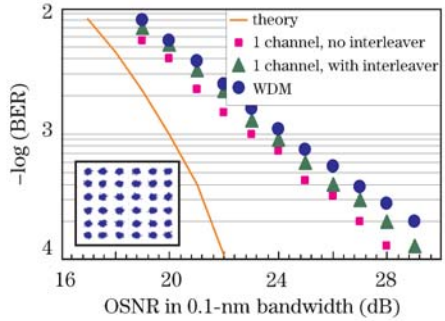

Fig. 5. BER curves and the corresponding constellation diagram for the performance of back-to-back.

and thus reduce the signal-to-noise ratio (SNR). For comparison, the electrical waveforms without and with pre-equalization are shown in Figs. 3(a) and (c), respectively. To confine the signal spectrum and reduce dense WDM (DWDM) crosstalk from the neighboring channels, raised cosine pulse shaping with a roll-off factor $b = 0.9$ is used for the baseband 36QAM signal. After electrical-to-optical conversion, polarization-multiplexing is achieved by dividing and recombining the signal with a 161-symbol delay before a polarization beam combiner. The optical spectra of the 36QAM optical signal before and after passing through 12.5-GHz optical interleaver are shown in Fig. 4. It is seen that the optical components have no much change after the interleaver. At the receiver, the measured signal is selected via a tunable optical filter (TOF) and a wavelength selected switch (WSS) with 0.5- and 0.1-nm bandwidths respectively and send to a real-time sampling scope for digital coherent detection. For the post-transmission digital signal processing (DSP), the 50-GSa/s signal is first down-sampled to 21.4 GSa/s (2×baud rate) after digital compensation of optical front-end errors (sampling skews and optical hybrid phase errors) and anti-aliasing filtering. After that, the chromatic dispersion (CD) is compensated using a finite impulse response (FIR) filter. Here, we employ three-stage equalization strategy: 1) the classic constant modulus algorithm (CMA) is used in the first stage to achieve pre-convergence; 2) the newly proposed cascaded multi-modulus algorithm (CMMA)[3,14,15] is used in the second stage to improve the SNR performance; 3) a decision-directed least-mean-square algorithm is applied in the third stage to further optimize the performance.

The measured back-to-back bit-error-rate (BER) performance as a function of OSNR is displayed in Fig. 5. The required OSNR in 0.1-nm noise bandwidth to achieve 2×10^{-3}BER for the single channel 107-Gb/s PDM-36QAM is 21 dB. The corresponding constellation diagram is inserted. There is a 0.5-dB OSNR penalty when the single channel passes through one 12.5-GHz optical interleaver, and a total OSNR penalty of ∼1 dB is caused when all WDM channels are turned on and passed through one 12.5-GHz optical interleaver.

2.4 64QAM format

One simple way to generate an eight-level electrical signal is using electrical coupler to combine three synchronized electrical signals with different amplitudes. However, due to reflection of these connectors of electrical cables and the coupler, it is very difficult to generate a high quality eight-level signals. Here we propose a novel scheme to generate high quality multi-level electrical signals[16,17]. The principle schematic is shown in Fig. 6. Three CW lightwaves are modulated by three individual intensity modulators (IMs) driven by different data (data A, B, and C). The powers of the optical signal of data A relative to those of data B and C are 3 and 6 dB larger, respectively, before they are combined by an optical coupler. The amplitude of optical signals can be adjusted by an optical attenuator. In order to synchronize these optical signals, optical time delays can be employed. Therefore, the generated eight-level optical signal is detected by a high-speed optical detector. By this way, the high quality eight-level electrical signal can be achieved. In order to get enough amplitude to drive I/Q modulator to generate 64QAM optical signal, the eight-level electrical signal from the optical detector can be boosted by an electrical amplifier. Obviously, the bit rate of the eight-level electrical signal is only limited by the bandwidth of these individual optical and electrical components such as IM, the electrical driver for IM, photodiode, and trans-impedance amplifier (TIA).

The experimental setup for 112.8-Gb/s PM-RZ-64QAM generation and detection is present in Fig. 7. We use one external cavity laser (ECL) at 1550.36 nm (full C-band tunable, linewidth of ∼100 kHz) to generate

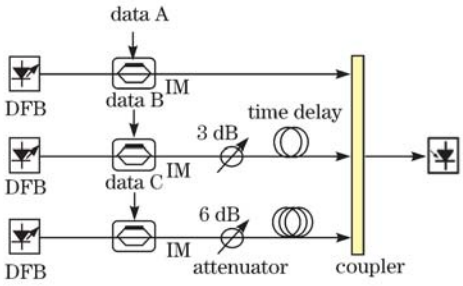

Fig. 6. Principle schematic for eight-level electrical signal generation. DFB: distributed feedback laser.

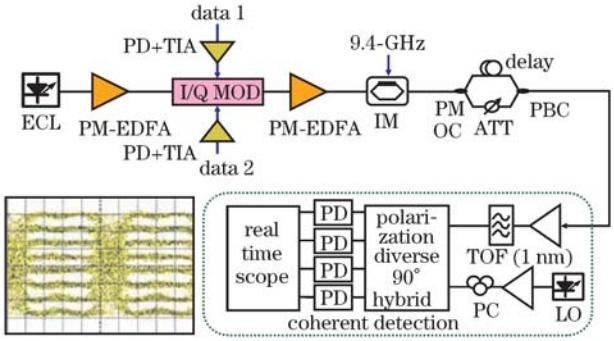

Fig. 7. Experimental setup for generation and detection of 112.8-Gb/s PM-RZ-64QAM optical signals. PD: photodetector; MDD: modulator; OC: optical coupler; ATT: attenuator; PC: polarization controller; LO: local oscillator.

CW lightwave. The 64QAM optical signal is generated by using a $\pi/2$-biased dual-parallel MZM (DP-MZM) driven by two eight-level electrical signals. The eye diagram of the electrical signal from the optical receiver is inserted in Fig. 7. There is a little distortion in the middle. The electrical amplitude from the optical receiver is 0.7 V (peak-to-peak p-p) when the input optical power is 0 dBm. Two eight-level electrical signals after different length fiber delays are used to drive the DP-MZM. Each modulator in the DP-MZM is biased at the null point. No booster amplifier is used to drive the DP-MZM. The half-wave electrical voltage of the modulator is 2.1 V. Because the modulators are driven at relatively low voltage, there is a large loss after passing through the DP-MZM. We use a PM-EDFA (EDFA: erbium-doped fiber amplifier) to boost the power of the CW lightwave from the ECL to 20 dBm. The optical power after the DP-MZM is −8 dBm. Then we employ another PM-EDFA to boost the optical power to 20 dBm. To introduce RZ-pulse shaping, an intensity MZM is added after the second PM-EDFA. The MZM intensity modulator is driven with a 9.4-GHz clock (to carve out $\sim$ 50% duty cycle pulses). This modulator is used to generate RZ pulses and change the spectral shape of the optical signal to increase the tolerance of the filtering effect. The polarization-multiplexing is achieved by dividing and recombining the signal with 150-symbol delay before a polarization beam combiner (PBC).

At the receiver, the local oscillator (LD) has a linewidth smaller than 400 Hz at 1550.36 nm. For the coherent receiver, polarization and phase-diverse coherent detection consists of a polarization-diverse 90° hybrid, one LO and four single-ended photodetectors. The distortion due to direct square-law detection of the signal component is mitigated by using a relatively high LO-to-signal power ratio (20 dB in this experiment) combined with a recently proposed DSP algorithm[14]. The LO is within 10 MHz of the transmit laser. The sampling and digitization (analog-to-digital, A/D) function is achieved by using a 4-channel digital storage scope with 50-Gs/s sampling rate and 9-GHz electrical bandwidth. The captured data are then post-processed using a desktop computer.

For the DSP, electrical polarization recovery is achieved by using a three-stage blind equalization strategy: we first use the classic constant modulus algorithm[2] for first pre-equalization, and then use the recently proposed CMMA[14] (for simplicity, only the inner three circles are used for error signal calculation) for second pre-equalization and finally we switch to the classic decision-directed least-mean square algorithm for final equalization. Carrier frequency, and phase recovery is achieved by using a maximum likelihood estimation algorithm based on the known constellation. For this experiment, errors were counted over 12×10^6 bits.

Figure 8 shows the measured BER performance of the RZ-64QAM optical signal. The measured constellation diagram of the generated single-polarization 64QAM optical signal with highest OSNR (44 dB) is inserted in Fig. 8. From Fig. 8, we can see that the required OSNRs at a BER of 2×10^{-3} (forward error correction (FEC) limitation) for the single and dual-polarization is 21 and 26.5 dB, respectively. The measured lowest BER for single polarization is 6×10^{-6}. We observe an excess 2.5-dB

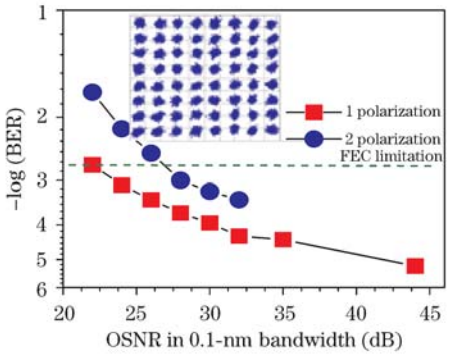

Fig. 8. BER performance of the RZ-64 QAM optical signal. Insert: constellation diagram of single-polarization 56.4-Gb/s 64QAM.

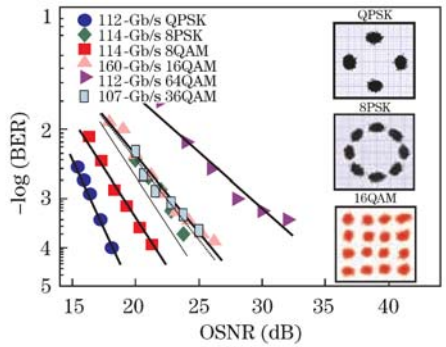

Fig. 9. Received OSNR in 0.1-nm bandwidth of different modulation formats. The back-to-back constellations of 112-Gb/s QPSK, 114-Gb/s 8PSK, and 160-Gb/s 16QAM are inserted.

polarization multiplexing penalty. This excess penalty should be reduced with advanced DSP.

2.5 OSNR of different formats

Figure 9 exhibits the measured BER versus OSNR curves for different modulation formats with the corresponding constellation maps. The required OSNRs at BER of 2×10^{-3} are 15.4[17], 21[17], 17.9, 22, 21.2, and 26.4 dB for 112-Gb/s QPSK, 114-Gb/s 8PSK, 114-Gb/s 8QAM, 160-Gb/s 16QAM, 107-Gb/s 36QAM, and 112-Gb/s 64QAM, repetitively. With digital coherent detection, PDM-QPSK has the benefits on lower OSNR requirement and simple transmitter configuration[17,18]. 16QAM should have lower OSNR requirement for 100-Gb/s signal, however, the measured signals work at 160-Gb/s, so the OSNR requirement is similar to 107-Gb/s PDM-36QAM. 8PSK should have better OSNR performance compared with 36QAM, but our measurement shows that the performance is close. It means that there are more margins to be obtained for 8PSK signal.

3. Ultra-capacity transmission experiment for 100 Gb/s

By employing these advanced modulation formats mentioned in above sections, a lot of high capacity transmission experiments have been demonstrated and published in top conferences such in recent years. These records include the largest capacity of 69.1 Tb/s in single fiber, the highest spectral efficiency (8 (bit/s)/Hz) for 100-Gb/s, 64-Tb/s capacity transmission.

To generate QPSK signal has the simplest configuration relative to other multilevel modulation format, but it has low spectral efficiency. We investigated the filtering effect for 100-Gb/s QPSK signal, and found that 25-GHz channel spacing is good enough for 112-Gb/s PDM-RZ-QPSK signal by using proper RZ pulse shape. We have demonstrated hybrid 112-Gb/s PDM-RZ-QPSK and 44-Gb/s PDM-NRZ-QPSK (NRZ: non-return-to-zero) transmission over 1600-km SMF-28 with pure EDFA amplification[18,19]. In this experiment, we built two 112-Gb/s PDM-RZ-QPSK transmitters and one 44-Gb/s PDM-NRZ-QPSK transmitter set. Each of the two 112-Gb/s transmitters modulates five 100-GHz spaced tunable ECLs with linewidth smaller than 100 kHz, while another ten 50-GHz spaced ECLs are modulated by the 44-Gb/s transmitter. The 10×112-Gb/s PDM-RZ-QPSK signals from two transmitters are combined first through a 50-GHz interleaver, and then the 10×44-Gb/s PDM-NRZ-QPSK signals are combined by a 25-GHz interleaver. Therefore, the channel spacing is 25 GHz for these twenty channels. Because the 44-Gb/s signal has better sensitivity (>5 dB) than the 112-Gb/s signal, the launch power of the 44-Gb/s signals is set 3 dB lower than that of the 112-Gb/s signals in order to reduce the crosstalk. The transmission line consists of 20 spans of 80-km standard single-mode fiber (SSMF, 17.3-dB average span loss) and EDFA-only amplification. No optical dispersion compensation is used. The total power launched into the transmission fiber is +12 dBm including 0 and −3 dBm for the 112- and 44-Gb/s channels, respectively. Here, we used coherent detection and off-line DSP to measure the BER performance. The measured OSNRs for the 112- and 44-Gb/s signals after transmission over 1600 km are 19 and 16 dB, respectively. BERs of all 100-Gb/s channels after transmission are in the range from 2×10^{-4} to 1.2×10^{-3}, which is under the FEC limitation, while the BERs for all 10×44-Gb/s channels are measured to be smaller than 1×10^{-5}. In the following sections we will present two high-capacity experiments which we achieved by using 8QAM and 36QAM modulation formats.

3.1 32-Tb/s (320×114-Gb/s) PDM-8QAM transmission[5]

Utilizing both C and L bands, here we report the successful transmission of 320×114-Gb/s DWDM signals over 580-km ultra-low-loss (ULL) SMF-28 fiber with a record information capacity of 32 Tb/s, without using Raman amplification, as shown in Fig. 10. The 8QAM modulator consists of a $\pi/4$-biased commercial DP-MZM with a 3-dB bandwidth about 19 GHz and a common (0, $\pi/2$) PM with a 3-dB bandwidth greater than 25 GHz. 8QAM modulator is driven by three 19-Gb/s binary electrical signals. To introduce ∼50% RZ-pulse shaping, a common MZM, MZM0, is added before the DP-MZM, driven by a 19-GHz sinusoidal clock. The generated 8QAM signal is then divided and recombined with about 1.6-ns time delay by using PBC to generate the required PDM-8QAM signal. Note that here we have added a C+L-band EDFA between the DP-MZM and the (0, $\pi/2$) PM. For this DWDM experiment, we built two transmitters, one for the 160 C+L-band odd wavelength channels and the other for the 160 C+L-band even channels. The sources of the 320 channels are all from conventional DFB lasers (linewidth ∼5 MHz). Due to the phase noise of the DFB lasers, the selected channel is switched from the DFB source to a tunable ECL source during each measurement. In the two transmitters we use polarization-maintaining C/L combiners, optical couplers, and C-band EDFAs; the L-band EDFAs are not polarization maintaining (due to availability), requiring polarization controllers (PCs) before the PMs. The transmission line consists of 7 spans of SMF-28 ULL fiber (82.8-km average length) and EDFA-only optical amplification. At 1550 nm, the measured average fiber loss is 0.169 dB/km (14.6 dB/span with connector loss included) and the average dispersion is 15.9 or 17.6 ps/(nm·km) at 1580 nm. The total launch power into the transmission fiber is 20 dBm (17 dBm for both the C-band and the L-band), corresponding to −5 dBm per channel. At such a launch power, stimulated Raman scattering introduces 2.5-dB/span gain tilt across the C+L bandwidth. This Raman tilt is compensated every span by introducing an opposite EDFA tilt through a mid-stage variable attenuator. For the 580-km transmission link, the measured total link PMD is 0.485 ps.

The measured BERs for all the 320 channels are shown in Fig. 11(a), where the inset shows the received constellation diagrams at 1539.97 nm, which is among the worst performing channels. It can be seen that all 320 channels have a BER below the enhanced FEC threshold 2×10^{-3}. In Figs. 11(b) and (c), we show the measured optical spectra of the modulated 320-channel signal before and

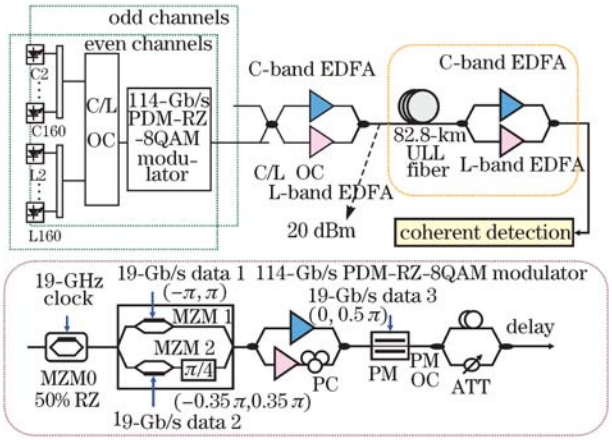

Fig. 10. Experimental setup for 32-Tb/s C+L-band transmission experiment.

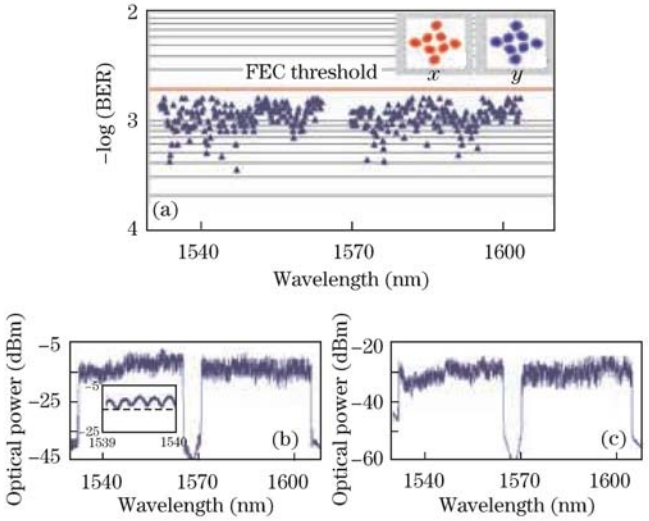

Fig. 11. Experimental results for 32-Tb/s transmission. (a) Measured BERs for 320 channels after 580-km transmission. The inset shows the received constellation diagram at 1539.97 nm. Monitored optical spectra for 320 channels (b) before and (c) after transmission (bandwidth 0.1 nm).

after transmission, respectively. The transmitted OSNRs in 0.1-nm noise bandwidth at 1532.4 (the shortest wavelength), 1564.07, 1569.94, and 1603.3 nm (the longest wavelength) are 29.9, 34, 31, and 30.5 dB, respectively. After 580-km transmission, the OSNRs decrease to 22.1, 24.8, 24.1, and 23.6 dB, accordingly.

3.2 64-Tb/s (640×107-Gb/s) PDM-36QAM transmission[3]

The experimental setup is shown in Fig. 12. It includes two transmitters, one for the 320 C+L-band odd wavelength channels and the other for the 320 C+L-band even channels. The 25-GHz-spaced odd and even channels are combined with a 12.5-GHz interleaver. For each of the two transmitters, we use 160 50-GHz-spaced conventional DFB sources to generate 320 25-GHz-spaced wavelength signals with carrier-suppressed tone-generation. By driving a MZM with a 12.5-GHz clock, we can generate two 25-GHz-spaced wavelength signals that are offset by +/−12.5-GHz from the original wavelength. The unwanted component located at the original carrier wavelength (at zero offset) as well as those located 25 GHz away from the original signal will be removed by the 12.5-GHz interleaver. But the spectral components located at 37.5 GHz away just fall within the same odd (or even) channels and become a source of crosstalk. Here this crosstalk is suppressed more than 30 dB by reducing the driving voltage and operating the MZM closer to the linear region. Such an under-driven condition introduces about 3 dB additional power loss. The 36-QAM optical signal is generated by driving an I/Q modulator with a 10.7-Gbaud 36QAM baseband signal obtained from a commercial AWG running at 21.4 GS/s. Because the phase noise of DFB lasers is too large for 36QAM modulation, an extra C+L-band tunable ECL with linewidth ∼ 100 kHz is introduced for BER measurement: the selected channel is sourced by the ECL instead of the DFB for each measurement. The line system consists of four 80-km spans of ultra-large-area fiber (ULAF), and the average fiber loss, dispersion, and dispersion slope at 1550 nm are 0.179 dB/km, 20.3 ps/(nm·km), 0.06 ps/(nm^2·km), respectively. The effective area is 127 μm^2. Hybrid EDFA/Raman optical amplifications with average Raman gain of about 5 dB across the C- and L-band are used to compensate the fiber span losses. For every span, two-stage C- and L-band EDFAs with mid-stage adjustable tilt filters are used to provide flat gain to compensate the span loss. The total launch power into the transmission fiber is 23.5 dBm, corresponding to −4.5 dBm/ch.

At the receiver, the measured channel is selected by a 12.5-GHz interleaver with two C+L-band tunable filters, TOF1 (0.3 nm) and TOF2 (1 nm). Polarization- and phase-diverse intradyne detection employs a polarization-diverse 90° hybrid, a tunable ECL LO (linewidth ∼100 kHz) and four balanced photo-detectors (for each measurement, the LO is tuned with ±50 MHz of the received signal center frequency). The sampling and ADC function is performed by a 4-channel real-time sampling scope with 50-GSa/s sampling rate and 16-GHz analog bandwidth. The captured data are then post-processed using a desktop computer.

For the post-transmission DSP, the 50-GSa/s signal is first down-sampled to 21.4 GSa/s (2 × baud rate)

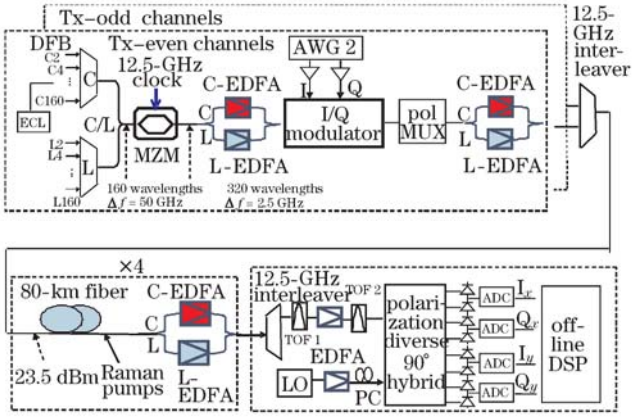

Fig. 12. Experimental setup for 64-Tb/s PDM-36QAM transmission. Tx: transmitter; Pol MUX: polarization multiplexer; ADC: analog-to-digital converter.

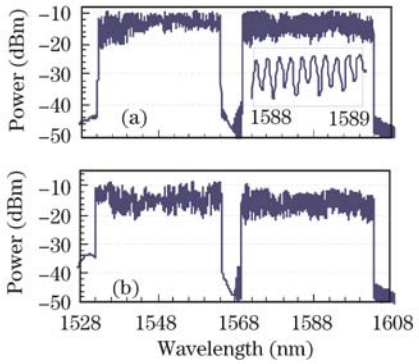

Fig. 13. (a) Launch and (b) received optical spectra of the 64-Tb/s transmission experiment.

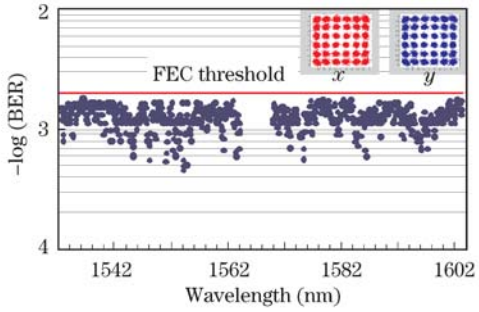

Fig. 14. BER performance after 320-km transmission.

after digital compensation of optical front errors (sampling skews and hybrid phase errors) and anti-aliasing filtering. After that, the CD is compensated using a fixed $T/2$-spaced FIR filter with 36 complex-valued taps. Next, we perform simultaneous polarization recovery and residual CD compensation with four complex-valued, 13-tap, $T/2$-spaced adaptive FIR filters, optimized by a three-stage equalization strategy: the classic CMA is used in the first stage to achieve pre-convergence, the newly proposed CMMA[14] is used in the second stage to improve the SNR performance, and finally a decision-directed least-mean-square algorithm is applied in the third stage to further optimize the performance. Note that carrier frequency and phase recoveries are implemented after the second equalization stage, and the frequency offset between the LO and the signal, as well as the carrier phase noise, is estimated using a constellation-assisted maximum likelihood estimation method[8]. For BER calculation, a quadrant-based differential decoding technique[9] is used to solve the $\pi/2$ phase ambiguity problem and errors are counted over 1.0×10^6 bit of information.

The results for the 64-Tb/s transmission experiment are shown in Figs. 13 and 14. In Figs. 13(a) and (b), we show the measured optical spectra (measured in 0.1-nm bandwidth) of the 640-channel signals before and after transmission, respectively. The transmitted OSNRs in 0.1-nm noise bandwidth at 1532.36 (the shortest wavelength), 1564.26, 1569.82, and 1603.30 nm (the longest wavelength) are 29.8, 31.6, 29, and 29.2 dB, respectively. After 320-km transmission, the OSNRs decreases to 24.6, 26.2, 25.4, and 24.6 dB, respectively. The measured BERs (average of both x- and y-polarization) for all 640 channels are shown in Fig. 14, where the inset shows the received constellation diagrams at 1602 nm, which is among the worst performing channels. As shown in Fig. 14, all 640 channels have a BER below the enhanced FEC threshold of 2×10^{-3}.

4. Conclusion

We demonstrate a few novel schemes to generate 8QAM, 16QAM, 36QAM, and 64QAM optical signals. For 8QAM, we employ a commercial dual-parallel DP-MZM followed by a common phase modulator with binary electrical driving signal through a novel synthesis technique. This 8QAM signal shows higher receiver sensitivity compared with 8PSK signal. We use three cascaded modulators driven by binary electrical signals to generate 16QAM optical signal. Different from other schemes to generate 16QAM, our components are all commercial and have good performance. We use pre- and post-digital equalization techniques to generate high performance 36QAM optical signal even if the bandwidth of the AWG is quite limited. For 64QAM signals, we employ the proposed new eight-level electrical signal generation scheme. The required OSNRs at BER of 2×10^{-3} are 15.4, 21, 17.9, 22, 21.2, and 26.4 dB for 112-Gb/s QPSK, 114-Gb/s 8PSK, 114-Gb/s 8QAM, 160-Gb/s 16QAM, 107-Gb/s 36QAM, and 112-Gb/s 64QAM, repetitively.

Additionally, we present the two large capacity and high-speed DWDM transmission experiments recently demonstrated using multi-level, multi-dimensional coding, and digital coherent detection. The first experiment demonstrates 32-Tb/s optical signal transmission over 580-km ULL fiber without Raman amplification by using PDM-8QAM modulation and coherent detection. At the second experiment, we demonstrate the highest spectral efficiency for 100-Gb/s signal transmission over 320-km fiber with a capacity of 64-Tb/s and PDM-36QAM modulation. These experimental results show that the high spectral efficiency and large capacity optical signal transmission can be realized by using these advanced multi-level modulation formats and coherent detection techniques.

Authors would like to thank T. Wang, M. Huang, and D. Qian from NEC Labs America for their support.

Most work in this publication was done in NEC Labs America and AT & L labs.

This work was partly supported by the National "863" Project of China (No. 2009AA01Z221) and the National "973" Project of China (No. 2010CB328300).

References

1. J. Yu, X. Zhou, M.-F. Huang, Y. Shao, D. Qian, T. Wang, M. Cvijetic, P. Magill, L. Nelson, M. Birk, S. Ten, H. B. Matthew, and S. K. Mishra, in *Proc. ECOC 2008* PDP Th.3.E.2 (2008).
2. X. Zhou, J. Yu, D. Qian, T. Wang, G. Zhang, and P. Magil, presented at the *OFC 2008* PDP1 (2008).
3. X. Zhou, in *Proc. OFC 2010* PDPB9 (2010).
4. A. Sano, in *Proc. OFC 2010* PDPB7 (2010).
5. J.-X. Cai, Y. Cai, C. R. Davidson, D. G. Foursa, A. Lucero, O. Sinkin, W. Patterson, A. Pilipetskii, G. Mohs, and N. S. Bergano, in *Proc. OFC 2010* PDPB10 (2010).

6. X. Zhou, J. Yu, M.-F. Huang, Y. Shao, T. Wang, P. Magill, M. Cvijetic, L. Nelson, M. Birk, G. Zhang, S. Ten, H. B. Matthew, and S. K. Mishra, in *Proc. OFC 2009* PDPB4 (2009).
7. A. H. Gnauck, G. Charlet, P. Tran, P. J. Winzer, C. R. Doerr, J. C. Centanni, E. C. Burrows, T. Kawanishi, T. Sakamoto, and K. Higuma, in *Proc. OFC 2007* PDP19 (2007).
8. G. Charlet, J. Renaudier, H. Mardoyan, P. Tran, O. B. Pardo, F. Verluise, M. Achouche, A. Boutin, F. Blache, J. Dupuy, and S. Bigo, in *Proc. OFC 2008* PDP3 (2008).
9. J. Yu, X. Zhou, and M. F. Huang, IEEE Photon. Technol. Lett. **21,** 1299 (2009).
10. X. Zhou, J. Yu, M.-F. Huang, Y. Shao, T. Wang, P. Magill, M. Cvijetic, L. Nelson, M. Birk, G. Zhang, S. Ten, H. B. Matthew, and S. K. Mishra, J. Lightwave Technol. **28,** 456 (2010).
11. A. H. Gnauck, P. J. Doerr, and L. L. Buhl, in *Proc. OFC 2009* PDPB8 (2009).
12. M. Nakazawa, in *Proc. ECOC 2008* Tu1.E.1 (2008).
13. X. Zhou and J. Yu, in *Proc. ECOC 2009* 10.3.5 (2009).
14. X. Zhou, J. Yu, and P. Magill, in *Proc. OFC 2009* OWG3 (2009).
15. X. Zhou and J. Yu, J. Lightwave. Technol. **27,** 3641 (2009).
16. J. Yu, X. Zhou, S. Gupta, Y.-K. Huang, and M.-F. Huang, IEEE Photon. Technol. Lett. **22,** 115 (2009).
17. J. Yu and X. Zhou, IEEE Commun. Magazine **48,** (3) S56 (2010).
18. J. Yu and X. Zhou, Opt. Fiber Technol. **15,** 197 (2009).
19. J. Yu, X. Zhou, M. F. Huang, D. Qian, L. Xu, and P. N. Ji, in *Proc. OFC 2009* OThR3 (2009).